

# Explore The Axion Dark Matter Through The Radio Signals From Magnetic White Dwarf Stars

Jin-Wei Wang<sup>a,b,c,¶</sup>, Xiao-Jun Bi<sup>d,e,†</sup>, Run-Min Yao<sup>d,e,‡</sup>, Peng-Fei Yin<sup>d,§</sup>

<sup>a</sup> *Scuola Internazionale Superiore di Studi Avanzati (SISSA), via Bonomea 265, 34136 Trieste, Italy*

<sup>b</sup> *INFN, Sezione di Trieste, via Valerio 2, 34127 Trieste, Italy*

<sup>b</sup> *Institute for Fundamental Physics of the Universe (IFPU), via Beirut 2, 34151 Trieste, Italy*

<sup>d</sup> *Key Laboratory of Particle Astrophysics, Institute of High Energy Physics, Chinese Academy of Sciences, Beijing, China*

<sup>e</sup> *School of Physical Sciences, University of Chinese Academy of Sciences, Beijing, China*

Axion as one of the promising dark matter candidates can be detected through narrow radio lines emitted from the magnetic white dwarf stars. Because of the existence of the strong magnetic field, the axion may resonantly convert into the radio photon (Primakoff effect) when it passes through the corona of the magnetic white dwarf, where the photon effective mass is equal to the axion mass. We show that for the magnetic white dwarf WD 2010+310, the future experiment SKA phase 1 with 100 hours of observation will set an upper limit on the axion-photon coupling  $g_{a\gamma}$  of  $\sim 10^{-12} \text{ GeV}^{-1}$  for the axion mass range of  $2 \times 10^{-8} \sim 10^{-6} \text{ eV}$ .

---

¶ jinwei.wang@sissa.it

† bixj@ihep.ac.cn

‡ yaorunmin@ihep.ac.cn

§ yinpf@ihep.ac.cn

# Contents

1	Introduction	2
2	The corona of the magnetic white dwarf and its magnetic field structure	3
3	The axion-photon conversion probability in the magnetosphere of the magnetic white dwarf	4
4	The radio flux density from the magnetic white dwarf	6
5	Conclusions	10

## 1 Introduction

The existence of dark matter (DM) has been established by solid astrophysical and cosmological observations [1,2]. For quite a long time the weakly interacting massive particles (WIMPs) are regarded as the most promising DM candidates, because they can naturally explain the DM relic density [3–5]. However, so far no convincing dark matter signal has been found in the direct detection, indirect detection, and collider detection experiments. Furthermore, the limitations on the couplings between the DM particles and standard model particles are becoming more and more stringent [4,6,7]. In this case, the experimental searches for other DM candidates have thus attracted increasingly attention in recent years [8,9].

Among many other alternatives, the QCD axion, a light neutral pseudoscalar particle associated with the  $U(1)$  Peccei-Quinn symmetry [10], is one of the best options due to several excellent theoretical characteristics: (1) it can resolve the strong CP problem very well [11–13]; (2) it can explain the observed DM abundance [14–16]. For more details we refer the reader to the excellent reviews of axion physics [17–19].

Based on the possible couplings between axion and the electromagnetic sector, a number of experiments have been set up to search for axion DM signals. These interactions predict two different phenomena: (1) the conversion between an axion particle and a photon under magnetic fields (so-called Primakoff effect [20]), e.g. axion helioscope [21,22], "light shining through a wall" experiments [23,24], and so on; (2) the photon birefringence under axion background [25–29]. In this paper we focus on the former phenomenon.

The compact stars, e.g. magnetic white dwarf stars (MWDs) and neutron stars, are very promising probes to search for the axion DM, since these stars host strong magnetic fields, in which the axion can be converted into detectable photon signals. For example, there are studies in the literature using the X-ray observations of MWDs to detect the star-born axions [30] and detecting the radio signals from axion DM conversion in the magnetospheres of neutron stars [31–34].

In this work we focus on the signals of axion DM from MWDs whose magnetic fields are at order of  $10^7 \sim 10^8$  G. With such a strong magnetic field, the axion DM may be converted into photons within the coronae of these MWDs. With the number density of plasma at the base of the MWD corona  $\sim 10^{10} \text{ cm}^{-3}$ , the effective photon mass  $m_\gamma$  in the corona is  $\sim \mu\text{eV}$ , which corresponds to a frequency of  $\sim \text{GHz}$ . This means that the axion DM with mass of  $m_a \sim \mu\text{eV}$  could fulfill the resonant conversion condition  $m_a \sim m_\gamma$  and thus the conversion probability can be enhanced greatly. The frequency of the corresponding signal happens to be in the sensitive region of the terrestrial radio telescopes, such as the Square Kilometer Array (SKA) that partially covers the  $50 \sim 1760$  MHz frequency band [35]. Therefore, we propose to use the radio telescopes to search for the axion DM in this mass range. Thus proposal can be regarded as a good supplement to the other axion detection experiment, such as ADMX [36–38] and CAST [21, 39, 40].

This paper is outlined as follows. In Sec. 2 we introduce the distribution of plasma density in the coronae of the MWDs and their magnetic field structure. In Sec. 3 we give a brief calculation of axion-photon conversion probability in the magnetic fields of MWDs. In Sec. 4 we calculate the radio flux density of some MWDs candidates as well as the constraints on the axion-photon coupling strength  $g_{a\gamma}$  at the SKA. Conclusions and further discussions are given in Sec. 5.

## 2 The corona of the magnetic white dwarf and its magnetic field structure

The X-radiation search can be used to set stringent constraints on the parameters of the MWDs' coronae [41, 42], which is suggested by several theories [43–45]. For example, the Chandra observation of the single cool MWD GD 356 sets limits on the plasma density of the hot corona as  $n_{e0} < 4.4 \times 10^{11} \text{ cm}^{-3}$  with the temperature of corona  $T_{\text{cor}} \sim 10^7$  K [42], while in Ref. [41] the upper limit on the plasma density is  $n_{e0} \sim 10^{10} \text{ cm}^{-3}$  with  $T_{\text{cor}} \gtrsim 10^6$  K for the MWD G99-47 (WD 0553+053). In the following sections, we show that the MWDs satisfying these constraints can be promising probes to detect the axion DM.

In this work, for the properties of the MWDs' coronae, we adopt the same assumptions as in Ref. [41]: (1) the corona is composed of fully ionized hydrogen plasma uniformly covering the entire surface of the white dwarf; (2) the field-aligned temperature of the electrons  $T_{\text{cor}} \sim 10^6$  K is a constant throughout the corona. Under these conditions the distribution of the electron density at  $r$  is described by the barometric formula [41, 42]

$$n_e(r) = n_{e0} \exp\left(-\frac{r - R_{\text{WD}}}{H_{\text{cor}}}\right), \quad (1)$$

where  $n_{e0}$  is the density at the base of the corona,  $R_{\text{WD}}$  is the radius of the MWDs, and

$$H_{\text{cor}} = \frac{2k_{\text{B}}T_{\text{cor}}}{m_{\text{p}}g} = 21.90 \left( \frac{T_{\text{cor}}}{10^6 \text{ K}} \right) \left( \frac{M_{\text{WD}}}{M_{\odot}} \right) \left( \frac{R_{\text{WD}}}{10^4 \text{ km}} \right)^{-2} \text{ km} \quad (2)$$

is the scale height of the isothermal corona,  $k_{\text{B}}$  is the Boltzmann constant,  $m_{\text{p}}$  is the proton mass,  $g$  is the free-fall acceleration at the surface of MWDs,  $M_{\text{WD}}$  is the mass of the MWDs.

Highly MWDs may give a very complex magnetic field structure [46]. In this work, for simplicity we take the dipole configuration as in Ref. [30]:

$$\mathbf{B} = \frac{B_0}{2} \frac{R_{\text{WD}}^3}{r^3} \left( 3(\hat{\mathbf{m}} \cdot \hat{\mathbf{r}}) \hat{\mathbf{r}} - \hat{\mathbf{m}} \right) \quad \text{for} \quad r > R_{\text{WD}}, \quad (3)$$

where  $B_0$  is the value of the magnetic field at the MWDs' surface in the direction of the magnetic pole,  $\mathbf{m} = 2\pi B_0 R_{\text{WD}}^3 \hat{\mathbf{m}}$  is the magnetic dipole moment,  $\mathbf{r} = r\hat{\mathbf{r}}$  is the spatial coordinate, and  $r = |\mathbf{r}|$  represents the distance from the center of the MWDs. Furthermore, we simply set  $\theta = \pi/2$  and expect that this assumption would give a satisfactory estimation. Then eq. (3) can be rewritten as a simpler form

$$B = |\mathbf{B}| = \frac{B_0}{2} \frac{R_{\text{WD}}^3}{r^3} \quad \text{for} \quad r > R_{\text{WD}}. \quad (4)$$

### 3 The axion-photon conversion probability in the magnetosphere of the magnetic white dwarf

In this section we present a more general formalism to calculate the axion-photon conversion probability in the magnetic fields of MWDs. The general interactions between axion and photon are given by the following Lagrangian [30]:

$$\begin{aligned} \mathcal{L} = & \frac{1}{2}(\partial_{\mu}a)^2 - \frac{1}{2}m_a^2 a^2 - \frac{1}{4}F_{\mu\nu}F^{\mu\nu} + \frac{1}{2}m_A^2 A_{\mu}A^{\mu} \\ & - \frac{1}{4}g_{a\gamma\gamma} a F_{\mu\nu}\tilde{F}^{\mu\nu} + \frac{\alpha_{\text{em}}^2}{90 m_e^4} \left[ (F_{\mu\nu}F^{\mu\nu})^2 + \frac{7}{4}(F_{\mu\nu}\tilde{F}^{\mu\nu})^2 \right], \end{aligned} \quad (5)$$

where  $a$  represents the axion field with the mass  $m_a$ ,  $F_{\mu\nu}$  is the electromagnetic field tensor,  $\tilde{F}^{\mu\nu} \equiv \frac{1}{2}\epsilon^{\mu\nu\rho\sigma}F_{\rho\sigma}$  is its dual,  $m_A$  is the photon's effective mass<sup>1</sup>,  $g_{a\gamma\gamma}$  is the axion-photon coupling,  $\alpha_{\text{em}}$  is the electromagnetic fine structure constant, and  $m_e$  is the electron mass. In the nonrelativistic plasma with nonzero electron density  $n_e$ , the effective mass of the photon is given by  $m_A = \sqrt{4\pi\alpha_{\text{em}}n_e/m_e}$ . The last term in eq. (5) is the Euler-Heisenberg effective Lagrangian arising from the vacuum polarizability [48]. It describes the photon's self-interaction

<sup>1</sup>Here we have ignored the term  $A_{\mu}j^{\mu}$ , in which  $j^{\mu}$  is the electromagnetic current density, since its physical consequence has been replaced by the photon's effective mass  $m_A$  when photon propagates in the plasma [47].

in the limit where the photon's frequency is small in comparison with the electron mass  $m_e$ . Its contribution to the  $m_A$  is estimated as [49, 33]

$$Q_A^{\text{EH}} = \frac{7\alpha_{\text{em}}}{45\pi} \omega^2 \frac{B^2}{B_{\text{cri}}^2} \quad (6)$$

where  $B_{\text{cri}} \equiv m_e^2/e = 4.4 \times 10^{13}$  G is a critical field strength,  $\omega$  is the photon's frequency. For the MWDs considered in this work, the strength of the magnetic field is about  $10^7 \sim 10^8$  G (see Table.1), which indicates  $B^2/B_{\text{cri}}^2 \ll 1$ . Therefore, we can safely ignore the effects of the Euler-Heisenberg term.

As shown below, the resonant conversion between the axion and photon occurs when the photon's effective mass  $m_A$  is equal to the axion mass  $m_a$  as

$$m_\gamma^2(r) = 4\pi\alpha \frac{n_e(r)}{m_e} = m_a^2. \quad (7)$$

By solving the eq. (1) and eq. (7), the resonant conversion radius  $r_c$  can be expressed as

$$r_c = R_{\text{WD}} + 21.90 \times \left[ 2.634 + \ln \left( \frac{n_{e0}}{10^{10} \text{ cm}^{-3}} \right) + \ln \left( \frac{\mu\text{eV}^2}{m_a^2} \right) \right] \\ \times \left( \frac{T_{\text{cor}}}{10^6 \text{ K}} \right) \left( \frac{M_{\text{WD}}}{M_\odot} \right) \left( \frac{R_{\text{WD}}}{10^4 \text{ km}} \right)^{-2} \text{ km}. \quad (8)$$

The equation of motion for the axion and photon field can be derived by applying the variational principle to eq. (5):

$$\ddot{a} - \nabla^2 a + m_a^2 a = -g_{a\gamma\gamma} \dot{\mathbf{A}} \cdot \mathbf{B}, \quad (9)$$

$$\ddot{\mathbf{A}} - \nabla^2 \mathbf{A} + m_A^2 \mathbf{A} = g_{a\gamma\gamma} \dot{a} \mathbf{B} - g_{a\gamma\gamma} \nabla a \times \dot{\mathbf{A}}. \quad (10)$$

Here we have chosen the temporal gauge  $A_0 = 0$  and the Coulomb gauge  $\nabla \cdot \mathbf{A} = 0$ . Following [32, 49] we adopt the radial plane wave solution  $a(r, t) = ie^{i\omega t - ikr} \tilde{a}(r)$  and  $A_\parallel(r, t) = e^{i\omega t - ikr} \tilde{A}_\parallel(r)$ , where  $k = \sqrt{\omega^2 - m_a^2}$  represents the momentum of the axion. Note that we have temporarily ignored the damping effects of the outgoing photon wave [32] and will include this effect in the finally answer.

Plugging the above plane wave solutions into the eq. (9)~(10) and using the WKB approximation  $|\tilde{A}_\parallel''(r)| \ll k|\tilde{A}_\parallel'(r)|$  and  $|\tilde{a}''(r)| \ll k|a'(r)|$  near  $r_c$ , we can rewrite the above mixing equations into a more compact first-order ordinary differential equation [32, 49]

$$\left[ -i \frac{d}{dr} + \frac{1}{2k} \begin{pmatrix} m_a^2 - m_A^2 & -\Delta_B \\ -\Delta_B & 0 \end{pmatrix} \right] \begin{pmatrix} \tilde{A}_\parallel \\ \tilde{a} \end{pmatrix} = 0, \quad (11)$$

where  $\Delta_B = Bg_{a\gamma\gamma}\omega$ ,  $\omega = m_a/\sqrt{1 - v_c^2}$ . Using the successive approximation method with the initial conditions  $\tilde{A}_\parallel(R_{\text{WD}}) = 0$  and  $\tilde{a}(R_{\text{WD}}) = a_0$ , at the first order of  $\Delta_B$  the eq. (11) can be

solved as [32, 49]

$$p_{a\gamma}(r) = \left| i \int_{R_{\text{WD}}}^r dr' \frac{\omega B(r') g_{a\gamma\gamma}}{2k} \times e^{\frac{if(r')}{2k}} \right|^2, \quad (12)$$

where

$$f(r') = \int_{R_{\text{WD}}}^{r'} d\tilde{r} [m_a^2 - m_A^2(\tilde{r})]. \quad (13)$$

Since  $1/2k \ll 1$ , we can evaluate eq. (12) by the method of stationary phase. With the condition  $df(r')/dr' = 0$ , we get  $m_a^2 - m_A^2(r_c) = 0$ , which exactly is the resonant conversion condition mentioned in eq. (7). By explicitly performing the integral in eq. (12) and including the damping effect of the photon wave, the probability of the axion-photon conversion at finite  $r$  is given by [32]

$$p_{a\gamma}(r) \approx \frac{1}{2v_c^2} g_{a\gamma\gamma}^2 B(r_c)^2 L^2 \times G\left(\frac{r - r_c}{L}\right) \times \begin{cases} 1, & r < r_c \\ \frac{m_a v_c}{D(r)}, & r \geq r_c \end{cases}, \quad (14)$$

with  $L = \sqrt{2\pi r_c v_c / (3m_a)}$  and  $D(r) = \sqrt{\omega^2 - m_A^2}$ . The function  $G(x)$  is defined by

$$G(x) = \frac{\left(\frac{1}{2} + C(x)\right)^2 + \left(\frac{1}{2} + S(x)\right)^2}{2} \quad (15)$$

in terms of the Fresnel  $C$  and  $S$  integrals

$$C(x) = \int_0^x dt \cos(\pi t^2 / 2), \quad S(x) = \int_0^x dt \sin(\pi t^2 / 2). \quad (16)$$

The last term in eq. (14) represents the damping effect of the photon wave [32]. Consider that all the astrophysical objects we are considering are very far away from us, i.e.  $\sim 0.1$  kpc, so eq. (14) can be further simplified as<sup>2</sup>

$$p_{a\gamma}^\infty = \lim_{r \rightarrow \infty} p_{a\gamma}(r) \approx \frac{1}{2v_c} g_{a\gamma\gamma}^2 B(r_c)^2 L^2. \quad (17)$$

Here we have used the fact that  $\lim_{x \rightarrow \infty} G(x) = 1$  and  $\lim_{r \rightarrow \infty} m_a v_c / D(r) = v_c$ .

## 4 The radio flux density from the magnetic white dwarf

In this work we consider the following conversion picture: the axion DM particle starts out non-relativistic ( $\sim 10^{-3} c$ ) far away from the MWDs and is accelerated as it moves toward the

---

<sup>2</sup>We have compared the numerical solutions by solving eq. (11) with this analytic approximation, and we find that these two results matched very well.

MWDs, then it is converted into the photon in the MWDs' corone with a certain probability  $p_{a\gamma}^\infty$ . Besides, because of the high density of the MWDs, all the incident photons that are converted from axons will be totally reflected back out [32, 50].

Once converted, the outgoing photons can be absorbed or scattered in the MWDs' corone, which is characterized by opacity. There are two important processes: the inverse bremsstrahlung process and Compton scattering. The absorption and scattering rate are given as [50]

$$\Gamma_{\text{inv}} \approx \frac{8\pi n_e n_N \alpha^3}{3\omega^3 m_e^2} \left( \frac{2\pi m_e}{T_{\text{cor}}} \right)^{1/2} \log \left( \frac{2T_{\text{cor}}^2}{m_A^2} \right) (1 - e^{-\omega/T_{\text{cor}}}), \quad (18)$$

$$\Gamma_{\text{Com}} = \frac{8\pi \alpha^2}{3m_e^2} n_e, \quad (19)$$

where  $n_N$  is the number density of the charged ions<sup>3</sup>. Then the probability for the converted photons to be scattered or absorbed during the propagation can be expressed as

$$P_{s/a} \simeq \exp \left[ - \int_{R_{\text{WD}}}^{\infty} dr (\Gamma_{\text{inv}} + \Gamma_{\text{Com}}) \right]. \quad (20)$$

For the MWDs candidates in Table.1 we calculate that the  $P_{s/a}$  is  $\sim 0.004$ , this means that the corona of the MWD is optically thin and the scattering and absorption of the photons can be safely ignored. The radiated power  $\mathcal{P}$  in a solid angle  $d\Omega$  at  $r_c$  can be estimated as [32]

$$\frac{d\mathcal{P}}{d\Omega} \approx 2 \times p_{a\gamma}^\infty \rho_{\text{DM}}^{r_c} v_c r_c^2, \quad (21)$$

where  $\rho_{\text{DM}}^{r_c}$  is the DM mass density at  $r = r_c$ . The factor of two is from the fact that the DM may convert into photons either on its way in to or out of the resonant layer. In the limit  $v_0^2/(GM_{\text{WD}}/r_c) \ll 1$ , the  $\rho_{\text{DM}}^{r_c}$  can be expressed as

$$\rho_{\text{DM}}^{r_c} = \rho_{\text{DM}}^\infty \frac{2}{\sqrt{\pi}} \frac{1}{v_0} \sqrt{\frac{2GM_{\text{WD}}}{r_c}} + \dots, \quad (22)$$

where  $\rho_{\text{DM}}^\infty$  is the DM density at infinity  $\sim 0.3 \text{ GeV/cm}^3$  and  $v_0 \sim 200 \text{ km/s}$  is the DM virial velocity. The radio flux density at the Earth can be estimated as

$$S_{a\gamma} = \frac{d\mathcal{P}}{d\Omega} \frac{1}{\mathcal{B}d^2}, \quad (23)$$

where  $d$  represents the distance from the MWD to us,  $\mathcal{B} = \max\{B_{\text{sig}}, B_{\text{res}}\}$  is the optimized bandwidth,  $B_{\text{sig}} \sim v_0^2 m_a / (2\pi)$  is the signal bandwidth, which is determined by the velocity dispersion in the asymptotic DM distribution, and  $B_{\text{res}}$  is the telescope spectral resolution. It is worth noting that in general  $B_{\text{sig}}$  is smaller than  $B_{\text{res}}$  (see Table. 2).

---

<sup>3</sup>Since the plasma is electric neutral, so we have  $n_e = n_N$ .

Parameters and expected radio flux density of the MWDs

	$M_{\text{WD}} [M_{\odot}]$	$R_{\text{WD}} [R_{\odot}]$	$T_{\text{eff}} [\text{K}]$	$B [\text{MG}]$	$d_{\text{WD}} [\text{pc}]$	$S_{a\gamma} [\mu\text{Jy}]$
RE J0317-853	1.32	0.00405	30000	200	29.54	0.29
WD 2010+310	1	0.00643	19750	520	30.77	8.68
WD 1031+234	0.937	0.00872	20000	200	64.09	0.60
WD 1043-050	1.02	0.00787	16250	820	83.33	5.02
WD 1743-520	1.13	0.00681	14500	36	38.93	0.033

Table 1: MWDs that make good candidates for measurement of the axion-induced radio flux. The columns correspond to the star’s mass in solar masses, radius in solar radii, effective temperature in Kelvin, magnetic field strength in mega-Gauss, distance from Earth in parsecs, and predicted radio flux density in  $\mu\text{Jy}$ . Some typical parameters are taken as  $m_a = 10^{-6} \text{ eV}$ ,  $g_{a\gamma\gamma} = 10^{-12} \text{ GeV}^{-1}$ ,  $n_{e0} = 10^{10} \text{ cm}^{-3}$ ,  $T_{\text{cor}} = 10^6 \text{ K}$ , and  $\mathcal{B} = 3.9 \text{ kHz}$ . The parameters from observations were obtained by merging the catalogs in Refs. [51, 46, 52].

Using eq. (17), (21)  $\sim$  (23) we can calculate the radio flux density for specific MWDs. In Table.1 we list the parameters of five MWD candidates as well as their radio flux densities  $S_{a\gamma}$ . The following typical parameters are selected for the calculation:  $m_a = 10^{-6} \text{ eV}$ ,  $g_{a\gamma\gamma} = 10^{-12} \text{ GeV}^{-1}$ ,  $n_{e0} = 10^{10} \text{ cm}^{-3}$ ,  $T_{\text{cor}} = 10^6 \text{ K}$ , and  $\mathcal{B} = 3.9 \text{ kHz}$  (see Talbe. 2). All these results should be compared to the minimum detectable flux density of a radio telescope, such as SKA [35], which can be expressed as

$$S_{\text{min}} = \frac{\text{SEFD}}{\eta_s \sqrt{n_{\text{pol}} \mathcal{B} t_{\text{obs}}}} , \quad (24)$$

where

$$\text{SEFD} = 2k_B \frac{T_{\text{sys}}}{A_{\text{eff}}} \quad (25)$$

is the system-equivalent flux density,  $n_{\text{pol}} = 2$  is the number of polarization,  $t_{\text{obs}}$  is the observation time,  $\eta_s$  is the system efficiency,  $k_B$  is the Boltzmann constant,  $T_{\text{sys}}$  is the antenna system temperature, and  $A_{\text{eff}}$  is the antenna effective area of the array. In this work, we take  $\eta_s = 0.9$  for SKA [35]. The values of the telescope spectral resolution  $B_{\text{res}}$  for SKA are listed in Table.2.

Next we propose to use the SKA phase 1 (SKA1) as a benchmark to search for the radio signals converted from axion DM at MWDs. As shown in Table. 2, it consists of a low-frequency aperture array (SKA1-Low) and a middle frequency aperture array (SKA1-Mid) [35]. The SKA1-Low covers the (50, 350) MHz frequency band, while the SKA1-Mid actually covers six frequency bands: (350, 1050) MHz, (950, 1760) MHz, (1650, 3050) MHz, (2800, 5180) MHz, (4600, 8500) MHz, and (8300, 15300) MHz. However, considering the constraints of the resonant conversion condition  $m_A \sim m_a$  as well as the plasma density  $n_{e0} \lesssim 10^{10} \text{ cm}^{-3}$ , there will be an upper bound on the frequency of the photon  $\sim \text{GHz}$ . Therefore, we only need to use the first



Parameters and sensitivity of the SKA

Name	$f$ [MHz]	$B_{\text{res}}$ [kHz]	$\langle T_{\text{sys}} \rangle$ [K]	$\langle A_{\text{eff}} \rangle$ [m <sup>2</sup> ]	SEFD [Jy]	$S_{\text{min}}$ [ $\mu$ Jy]
SKA1-Low	(50, 350)	1	680	$2.2 \times 10^5$	8.54	353.42
SKA1-Mid B1	(350, 1050)	3.9	28	$2.7 \times 10^4$	2.86	60.04
SKA1-Mid B2	(950, 1760)	3.9	20	$3.5 \times 10^4$	1.58	33.09

Table 2: The frequency range, telescope spectral resolution  $B_{\text{res}}$ , averaged system temperature  $T_{\text{sys}}$ , averaged effective area  $A_{\text{eff}}$ , SEFD, and minimum detectable flux density in the different frequency bands for SKA1.

two frequency bands SKA1-Mid B1 and SKA1-Mid B2 in our analysis. The specific parameters of the different frequency bands of the SKA are listed in Table. 2.

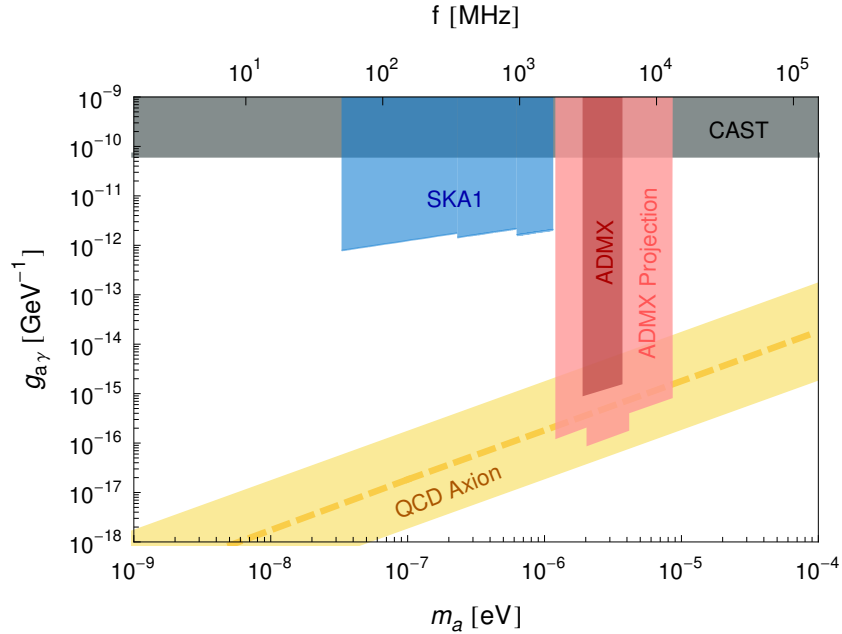


Figure 1: The projected sensitivity to  $g_{a\gamma}$  as a function of the axion mass  $m_a$  for SKA1 telescopes with 100 hours observations of the WD 2010+310. The QCD axion is predicted to lie within the yellow band. The limits set by CAST and ADMX (current and projected) are indicated by the gray and red regions, respectively.

In Fig. 1 we show the sensitivity to  $g_{a\gamma}$  for the WD 2010+310, which is the strongest source in Talbe. 1. The blue regions show the physics potential of SKA1 with 100 hours of observation. We find that the axion DM in the mass range of  $2 \times 10^{-8} \sim 10^{-6}$  eV can be probed effectively, and the limitation on  $g_{a\gamma}$  is about  $\lesssim 10^{-12}$  GeV<sup>-1</sup>. For comparison, the limitations given by the other two experiments, e.g. ADMX and CAST, are also shown in red and gray regions,

respectively.

## 5 Conclusions

In this work we propose to use MWDs as probes to detect the axion DM through the radio signals. It is known that the MWDs can host very strong magnetic field (e.g.  $10^7 \sim 10^8$  G). If we adopt the corona parameters that fulfill the X-ray constraints, such as  $n_{e0} \sim 10^{10} \text{ cm}^{-3}$  and  $T_{\text{cor}} \sim 10^6$  K, the effective photon mass is given by  $m_\gamma \sim \mu\text{eV}$  (corresponding to the frequency  $\sim$  GHz). We find that the resonant conversion may happen when axions pass through the magnetosphere that is a narrow region around the radius at which the photon effective mass is equal to the axion mass. Besides, we show that the effects of the inverse bremsstrahlung process and Compton scattering for the outgoing photons are negligible ( $P_{a/s} \sim 0.004$ ). Therefore, once converted, the radio photon can pass unimpededly through the MWDs' coronae and be detected by the radio telescope on Earth.

Meanwhile, it is intriguing that for the axion DM with mass  $\sim \mu\text{eV}$ , which happens to be in the sensitive region of the terrestrial radio telescopes, such as SKA. In Sec. 4 we use the MWD WD 2010+310 as a target and show the sensitivity to  $g_{a\gamma}$  from the future experiment SKA phase 1 with 100 hours of observation. We find that the planned SKA1 will give an upper limit on the axion-photon coupling  $g_{a\gamma}$  of  $\sim 10^{-12} \text{ GeV}^{-1}$  for axion mass range of  $2 \times 10^{-8} \sim 10^{-6}$  eV, and this result may increase by more than an order of magnitude in the SKA phase 2 (SKA2) [35, 33].

Note that all of the MWDs considered are isolated. In fact, one can consider another class of MWDs that occupy regions of high DM density and/or low velocity dispersion, such as the galactic center, dwarf galaxies, and so on. In these regions, the DM density may be enhanced by a large factor. In addition, in dwarf galaxies the velocity dispersion of DM can be low as  $v_0 \sim 10 \text{ km/s}$ . These cases would significantly improve our results and are left for the future work.

## Acknowledgements

The work of JWW is supported by the research grant "the Dark Universe: A Synergic Multimessenger Approach" number 2017X7X85K under the program PRIN 2017 funded by the Ministero dell'Istruzione, Università e della Ricerca (MIUR). The work of XJB, RMY, and PFY is supported by the National Key R&D Program of China (No. 2016YFA0400200), the National Natural Science Foundation of China (Nos. U1738209 and 11851303).

# References

- [1] D. Clowe, M. Bradac, A. H. Gonzalez, M. Markevitch, S. W. Randall, C. Jones, and D. Zaritsky, “A direct empirical proof of the existence of dark matter,” *Astrophys. J. Lett.* **648** (2006) L109–L113, [arXiv:astro-ph/0608407](#).
- [2] **Planck** Collaboration, N. Aghanim *et al.*, “Planck 2018 results. VI. Cosmological parameters,” *Astron. Astrophys.* **641** (2020) A6, [arXiv:1807.06209 \[astro-ph.CO\]](#).
- [3] G. Bertone, D. Hooper, and J. Silk, “Particle dark matter: Evidence, candidates and constraints,” *Phys. Rept.* **405** (2005) 279–390, [arXiv:hep-ph/0404175](#).
- [4] J. L. Feng, “Dark Matter Candidates from Particle Physics and Methods of Detection,” *Ann. Rev. Astron. Astrophys.* **48** (2010) 495–545, [arXiv:1003.0904 \[astro-ph.CO\]](#).
- [5] G. Arcadi, M. Dutra, P. Ghosh, M. Lindner, Y. Mambrini, M. Pierre, S. Profumo, and F. S. Queiroz, “The waning of the WIMP? A review of models, searches, and constraints,” *Eur. Phys. J. C* **78** (2018) 203, [arXiv:1703.07364 \[hep-ph\]](#).
- [6] J. Liu, X. Chen, and X. Ji, “Current status of direct dark matter detection experiments,” *Nature Phys.* **13** (2017) 212–216, [arXiv:1709.00688 \[astro-ph.CO\]](#).
- [7] L. Zhao and J. Liu, “Experimental search for dark matter in China,” *Front. Phys. (Beijing)* **15** (2020) 44301, [arXiv:2004.04547 \[astro-ph.IM\]](#).
- [8] G. Sigl and P. Trivedi, “Axion-like Dark Matter Constraints from CMB Birefringence,” [arXiv:1811.07873 \[astro-ph.CO\]](#).
- [9] G. Bertone *et al.*, “Gravitational wave probes of dark matter: challenges and opportunities,” [arXiv:1907.10610 \[astro-ph.CO\]](#).
- [10] R. Peccei and H. R. Quinn, “Constraints Imposed by CP Conservation in the Presence of Instantons,” *Phys. Rev. D* **16** (1977) 1791–1797.
- [11] R. D. Peccei and H. R. Quinn, “CP Conservation in the Presence of Pseudoparticles,” *Phys. Rev. Lett.* **38** (Jun, 1977) 1440–1443.
- [12] S. Weinberg, “A New Light Boson?,” *Phys. Rev. Lett.* **40** (Jan, 1978) 223–226.
- [13] F. Wilczek, “Problem of Strong  $P$  and  $T$  Invariance in the Presence of Instantons,” *Phys. Rev. Lett.* **40** (Jan, 1978) 279–282.
- [14] J. Preskill, M. B. Wise, and F. Wilczek, “Cosmology of the invisible axion,” *Physics Letters B* **120** (1983) 127 – 132.
- [15] L. Abbott and P. Sikivie, “A cosmological bound on the invisible axion,” *Physics Letters B* **120** (1983) 133 – 136.
- [16] M. Dine and W. Fischler, “The not-so-harmless axion,” *Physics Letters B* **120** (1983) 137 – 141.
- [17] P. W. Graham, I. G. Irastorza, S. K. Lamoreaux, A. Lindner, and K. A. van Bibber, “Experimental Searches for the Axion and Axion-Like Particles,” *Ann. Rev. Nucl. Part. Sci.* **65** (2015) 485–514, [arXiv:1602.00039 \[hep-ex\]](#).
- [18] L. Di Luzio, M. Giannotti, E. Nardi, and L. Visinelli, “The landscape of QCD axion models,” *Phys. Rept.* **870** (2020) 1–117, [arXiv:2003.01100 \[hep-ph\]](#).
- [19] D. J. E. Marsh, “Axion Cosmology,” *Phys. Rept.* **643** (2016) 1–79, [arXiv:1510.07633 \[astro-ph.CO\]](#).
- [20] H. Primakoff, “Photoproduction of neutral mesons in nuclear electric fields and the mean life of the neutral meson,” *Phys. Rev.* **81** (1951) 899.
- [21] **CAST** Collaboration, V. Anastassopoulos *et al.*, “New CAST Limit on the Axion-Photon Interaction,” *Nature Phys.* **13** (2017) 584–590, [arXiv:1705.02290 \[hep-ex\]](#).
- [22] E. Armengaud *et al.*, “Conceptual Design of the International Axion Observatory (IAXO),” *JINST* **9** (2014) T05002, [arXiv:1401.3233 \[physics.ins-det\]](#).

- [23] K. Ehret *et al.*, “New ALPS Results on Hidden-Sector Lightweights,” *Phys. Lett. B* **689** (2010) 149–155, [arXiv:1004.1313 \[hep-ex\]](#).
- [24] R. Bähre *et al.*, “Any light particle search II —Technical Design Report,” *JINST* **8** (2013) T09001, [arXiv:1302.5647 \[physics.ins-det\]](#).
- [25] W. DeRocco and A. Hook, “Axion interferometry,” *Phys. Rev. D* **98** (2018) 035021, [arXiv:1802.07273 \[hep-ph\]](#).
- [26] I. Obata, T. Fujita, and Y. Michimura, “Optical Ring Cavity Search for Axion Dark Matter,” *Phys. Rev. Lett.* **121** (2018) 161301, [arXiv:1805.11753 \[astro-ph.CO\]](#).
- [27] H. Liu, B. D. Elwood, M. Evans, and J. Thaler, “Searching for Axion Dark Matter with Birefringent Cavities,” *Phys. Rev. D* **100** (2019) 023548, [arXiv:1809.01656 \[hep-ph\]](#).
- [28] T. Fujita, R. Tazaki, and K. Toma, “Hunting Axion Dark Matter with Protoplanetary Disk Polarimetry,” *Phys. Rev. Lett.* **122** (2019) 191101, [arXiv:1811.03525 \[astro-ph.CO\]](#).
- [29] G.-W. Yuan, Z. Xia, C. Tang, Y. Zhao, Y.-F. Cai, Y. Chen, J. Shu, and Q. Yuan, “Testing the ALP-photon coupling with polarization measurements of Sagittarius A\*,” [arXiv:2008.13662 \[astro-ph.HE\]](#).
- [30] C. Dessert, A. J. Long, and B. R. Safdi, “X-ray signatures of axion conversion in magnetic white dwarf stars,” *Phys. Rev. Lett.* **123** (2019) 061104, [arXiv:1903.05088 \[hep-ph\]](#).
- [31] M. Pshirkov and S. Popov, “Conversion of Dark matter axions to photons in magnetospheres of neutron stars,” *J. Exp. Theor. Phys.* **108** (2009) 384–388, [arXiv:0711.1264 \[astro-ph\]](#).
- [32] A. Hook, Y. Kahn, B. R. Safdi, and Z. Sun, “Radio Signals from Axion Dark Matter Conversion in Neutron Star Magnetospheres,” *Phys. Rev. Lett.* **121** (2018) 241102, [arXiv:1804.03145 \[hep-ph\]](#).
- [33] F. P. Huang, K. Kadota, T. Sekiguchi, and H. Tashiro, “Radio telescope search for the resonant conversion of cold dark matter axions from the magnetized astrophysical sources,” *Phys. Rev. D* **97** (2018) 123001, [arXiv:1803.08230 \[hep-ph\]](#).
- [34] J. Darling, “Search for Axionic Dark Matter Using the Magnetar PSR J1745-2900,” *Phys. Rev. Lett.* **125** (2020) 121103, [arXiv:2008.01877 \[astro-ph.CO\]](#).
- [35] S. collaboration, “Ska1 system baseline design,” 2013. [https://www.skatelescope.org/wp-content/uploads/2014/11/SKA-TEL-SKO-0000002-AG-BD-DD-Rev01-SKA1\\_System\\_Baseline\\_Design.pdf](https://www.skatelescope.org/wp-content/uploads/2014/11/SKA-TEL-SKO-0000002-AG-BD-DD-Rev01-SKA1_System_Baseline_Design.pdf). document number: SKA-TEL-SKO-DD-001.
- [36] S. Asztalos, E. Daw, H. Peng, L. J. Rosenberg, C. Hagmann, D. Kinion, W. Stoeffl, K. van Bibber, P. Sikivie, N. S. Sullivan, D. B. Tanner, F. Nezrick, M. S. Turner, D. M. Moltz, J. Powell, M.-O. André, J. Clarke, M. Mück, and R. F. Bradley, “Large-scale microwave cavity search for dark-matter axions,” *Phys. Rev. D* **64** (Oct, 2001) 092003.
- [37] S. J. Asztalos, G. Carosi, C. Hagmann, D. Kinion, K. van Bibber, M. Hotz, L. J. Rosenberg, G. Rybka, J. Hoskins, J. Hwang, P. Sikivie, D. B. Tanner, R. Bradley, and J. Clarke, “SQUID-Based Microwave Cavity Search for Dark-Matter Axions,” *Phys. Rev. Lett.* **104** (Jan, 2010) 041301.
- [38] T. Shokair *et al.*, “Future Directions in the Microwave Cavity Search for Dark Matter Axions,” *Int. J. Mod. Phys. A* **29** (2014) 1443004, [arXiv:1405.3685 \[physics.ins-det\]](#).
- [39] CAST Collaboration, M. Arik *et al.*, “Search for Solar Axions by the CERN Axion Solar Telescope with  $^3\text{He}$  Buffer Gas: Closing the Hot Dark Matter Gap,” *Phys. Rev. Lett.* **112** (2014) 091302, [arXiv:1307.1985 \[hep-ex\]](#).
- [40] CAST Collaboration, M. Arik *et al.*, “New solar axion search using the CERN Axion Solar Telescope with  $^4\text{He}$  filling,” *Phys. Rev. D* **92** (2015) 021101, [arXiv:1503.00610 \[hep-ex\]](#).
- [41] V. V. Zheleznyakov, S. A. Koryagin, and A. V. Serber, “Thermal cyclotron radiation by isolated magnetic white dwarfs and constraints on the

- parameters of their coronas,” *Astronomy Reports* **48** (2004) 121–135.
- [42] M. C. Weisskopf, K. Wu, V. Trimble, S. L. O’Dell, R. F. Elsner, V. E. Zavlin, and C. Kouveliotou, “A Chandra Search for Coronal X-Rays from the Cool White Dwarf GD 356,” *The Astrophysical Journal* **657** (Mar, 2007) 1026–1036.
- [43] V. V. Zheleznyakov and A. A. Litvinchuk, “On the theory of cyclotron lines in the spectra of magnetic white dwarfs,” *Astronomy Reports* **105** (1984) 73–84.
- [44] A. V. Serber, “Transfer of Cyclotron Radiation in a Tenuous Collisional Plasma on a Magnetic White Dwarf,” *Soviet Astronomy* **34** (June, 1990) 291.
- [45] J. H. Thomas, J. A. Markiel, and H. M. van Horn, “Dynamo Generation of Magnetic Fields in White Dwarfs,” *Astrophysical Journal* **453** (Nov., 1995) 403.
- [46] L. Ferrario, D. de Martino, and B. Gaensicke, “Magnetic White Dwarfs,” *Space Sci. Rev.* **191** (2015) 111–169, [arXiv:1504.08072 \[astro-ph.SR\]](#).
- [47] P. Robles and F. Claro, “Can there be massive photons? A pedagogical glance at the origin of mass,” *European Journal of Physics* **33** (Jul, 2012) 1217–1226.
- [48] W. Heisenberg and H. Euler, “Dynamo Generation of Magnetic Fields in White Dwarfs,” *Zeitschrift für Physik* **98** (Nov., 1936) 714–732.
- [49] G. Raffelt and L. Stodolsky, “Mixing of the photon with low-mass particles,” *Phys. Rev. D* **37** (Mar, 1988) 1237–1249.
- [50] H. An, F. P. Huang, J. Liu, and W. Xue, “Radiofrequency Dark Photon Dark Matter across the Sun,” [arXiv:2010.15836 \[hep-ph\]](#).
- [51] S. Kleinman *et al.*, “SDSS DR7 White Dwarf Catalog,” *Astrophys. J. Suppl.* **204** (2013) 5, [arXiv:1212.1222 \[astro-ph.SR\]](#).
- [52] **Gaia** Collaboration, A. Brown *et al.*, “Gaia Data Release 2: Summary of the contents and survey properties,” *Astron. Astrophys.* **616** (2018) A1, [arXiv:1804.09365 \[astro-ph.GA\]](#).